# HRAM: Underwater Hierarchical Route Allocation Mechanism Based on Load Balancing

Na Liu
*College of Information Engineering*
*Yangzhou University*
Yangzhou, China
mx120220567@stu.yzu.edu.cn

Yi Jiang(✉)
*College of Information Engineering*
*Yangzhou University*
Yangzhou, China
jiangyi@yzu.edu.cn

Xinpeng Lu
*College of Information Engineering*
*Yangzhou University*
Yangzhou, China
211301216@stu.yzu.edu.cn

2024 IEEE International Conference on Cognitive Computing and Complex Data (ICCD) | 979-8-3503-5289-4/24/$31.00 ©2024 IEEE | DOI: 10.1109/ICCD62811.2024.10843414

***Abstract*—Underwater Wireless Sensor Networks are widely used in marine resource exploration and military device deployment. However, uneven network load and high node energy consumption severely hinder their practical applications. In this paper, we established a Hierarchical Underwater multi-hop Wireless Sensor Network model (HUWSN), which describes the data transmission process within the network. Based on the model, we proposed an underwater Hierarchical Route Allocation Mechanism (HRAM) aiming to achieve network load balancing. Specifically, t he m echanism fi rst ut ilized a Balanced Routing Selection Algorithm (BRSA) to form the initial network topology, ensuring a balanced distribution of relay tasks among layers. Subsequently, load distribution over network links was balanced by using the Data Allocation Algorithm based on load factor (DAA). Finally, the allocation of the amount of data in routing was optimized by using the Heuristic Route Allocation Optimization Algorithm (HRAOA). The experimental results showed that compared with existing methods, the proposed mechanism effectively reduces total energy consumption of nodes while maintaining a balanced network load.**

***Keywords*—*underwater wireless sensor networks*, *route allocation*, *load balancing*, *multi-hop transmission***

## I. Introduction

Underwater Wireless Sensor Networks (UWSNs) consist of a large number of sensor nodes that distributed throughout the underwater. They communicate with each other through wireless communication protocols, forming a self-organizing underwater monitoring network system [1]. The underwater system collects and transmits a variety of data, such as meteorological data, topography details, and environmental factors, to a base station located onshore. The base station possesses high computing and storage capabilities for processing the received information. It offers valuable data support for marine resource investigations [2], natural disaster prediction [3], as well as underwater pipeline monitoring [4]. However, due to the limited communication range of sensor nodes, they cannot directly transmit data to the base station. Relay nodes are therefore commonly utilized as relays for data transmission, sending information to the base station via multi-hop routing. Conventional sensor nodes are often low-energy efficient a nd d ependent o n a n e xternal power source. Moreover, wireless communication methods, such as acoustic or electromagnetic waves, typically exhibit limited communication bandwidth, thereby constraining the speed and efficiency of data transmission. These factors place certain limitations on sensor nodes in terms of energy consumption and data transmission. In contrast, Autonomous Underwater Vehicles (AUVs), as autonomous working nodes, are typically equipped with advanced communication devices. They possess higher communication bandwidth and transmission rates, consequently, utilizing AUVs as relay nodes can significantly enhance the stability and reliability of data transmission.

It's worth working on that UWSNs are different from Wireless Sensor Networks (WSNs) lies in the presence of phenomena such as sound wave reflection and refraction [5]. Additionally, underwater signal propagation is influenced by various factors including water absorption, scattering, and multi-path effects, which lead to signal attenuation and increased transmission delays. These phenomena result in a higher bit error rate and poorer quality of communication links in underwater [6]. Hence, UWSNs face a unique set of challenges: **on one hand**, the diverse sizes of data packets being forwarded by nodes result in a situation where the limited link bandwidth becomes a critical bottleneck. This limitation renders the network particularly vulnerable to congestion and causes uneven load distribution among the nodes [7]. Such congestion not only reduces the overall data transmission efficiency but also increases latency, making it difficult for time-sensitive applications, such as environmental monitoring or disaster response, to function optimally. **On the other hand**, unequal energy consumption among nodes is an inevitable issue in multi-hop routing. Nodes situated closer to the Sink, tend to experience a rapid depletion of their energy resources because they are responsible for forwarding a greater number of packets. This imbalanced energy expenditure leads to what is known as the hot spot problem [8]. As a result, nodes located within the Sink Connectivity Area (SCA) [1] face quicker energy depletion and ultimately failure.

Moreover, these challenges pose significant implications for existing routing protocols and data allocation strategies in UWSNs. Standard routing approaches might fail to provide equitable energy usage across the network, thus hastening the onset of the hot spot phenomenon. Building a routing

[1]The Sink Connectivity Area (SCA) is the aggregated region in UWSNs responsible for data transmission, typically located near the base station.

979-8-3503-5289-4/24/$31.00 ©2024 IEEE

solution that addresses both the bandwidth limitations and energy conservation needs is essential for enhancing the overall performance and longevity of UWSNs. In addition, traditional data distribution methods may not adequately account for the dynamic nature of packet sizes and the bandwidth of nodes, leading to suboptimal path selections that lead to uneven network loads.

Focusing on the route allocation problem in UWSNs, the proposed HRAM selects the optimal routing and data allocation strategies to achieve load balancing of data traffic across multiple paths, using heterogeneous AUVs as relay nodes. The main contributions are as follows:

- In terms of relay node selection, we propose a novel Balanced Routing Selection Algorithm (BRSA). It utilizes the evaluation function and path counter of nodes to construct a stable initial network topology. It carefully considers the capabilities and load-bearing potential of each node. By doing so, it avoids excessive routing burden on nodes within the same layer, which is a common problem in many traditional routing algorithms. In traditional approaches, nodes may be selected as relays without considering their current load or potential for handling additional traffic.
- To address the issue of data allocation, we propose a Data Allocation Algorithm based on load factor (DAA). By allocating data according to the status of relay nodes and link bandwidth, the algorithm mitigates traffic pressure and achieves load balancing across the network. This is a major departure from conventional algorithms that often allocate data without taking into account these critical factors. Traditional data allocation methods may lead to uneven distribution of data, resulting in some nodes being overloaded while others remain underutilized.
- The Heuristic Route Allocation Optimization Algorithm (HRAOA) is proposed to further optimize the amount of data allocation. By simulating the evolutionary process, HRAOA aims to search for an optimal routing scheme, which reduces the link load variance and overall energy consumption in the network. The HRAOA considers load balancing when forming the initial population, unlike other algorithms which may lead to suboptimal solutions. Moreover, with an improved fitness function and genetic operator, HRAOA achieves a more stable load variance in fewer iterations.

## II. Related Work

The UWSNs technology has attracted widespread attention both domestically and internationally, with many scholars conducting in-depth research in node location tracking [9], arrangement and networking [10], as well as routing protocols [11]. Route allocation in UWSNs involves considering the characteristics of nodes and resource constraints to obtain the optimal routing as well as reasonable allocation of data. Zhang [12] designed a non-uniform clustering method based on virtual gravitational potential energy to construct the optimal routing. Zhao [13] proposed an energy-efficient multi-level routing strategy based on reinforcement learning. Wang [14] defined the forwarding region so that nodes closer to the destination tend to forward. The forwarding dilemma game was used to find the optimal routing inside the forwarding region. Lin [15] established a Nash equilibrium for the energy balancing game by modeling the load allocation as a game model. It was developed to capture the behavior of actual sensors through a utility function.

These studies have shown that the field of optimal routing for UWSNs has been extensively investigated, yielding fruitful outcomes. However, certain challenges still remain to be addressed. When designing the routing, [12]–[14] did not consider the network load balancing. Additionally, the heterogeneity of nodes in the network was ignored, except for [13], [15]. While a study that considers the heterogeneity of nodes [15], paied attention to the energy balance among nodes, it neglected load balancing of links in the network.

**Brief Conclusion**. Unlike all the above scenarios on route allocation in UWSNs, we focus on the problem of load balancing and design the HRAM. The HRAM enhances the transmission performance of the network by ensuring a balanced distribution of data traffic across network links.

## III. System Model

### A. Model Description and Notations

We consider a Hierarchical Underwater multi-hop Wireless Sensor Network model (HUWSN) as shown in Fig.1. The HUWSN consists of $I$ sensor source nodes, $A$ AUVs, and a base station $Sink$. Let $\mathcal{I} = \{1, \cdots, i, \cdots, I\}$ and $\mathcal{A} = \{1, \cdots, a, \cdots, A\}$ denote the set of sensor source nodes and AUVs respectively. In the vertical direction, one layer is set for every $\delta$ meter [16]. The sensor source nodes are situated at the bottom layer of the underwater, heterogeneous AUVs are uniformly distributed in each intermediate layer, and the $Sink$ is located in the topmost layer. The layer below the $Sink$ is called SCA region. Nodes in this area are referred to hot spots and can communicate directly with the $Sink$, through which all other nodes transmit their data.

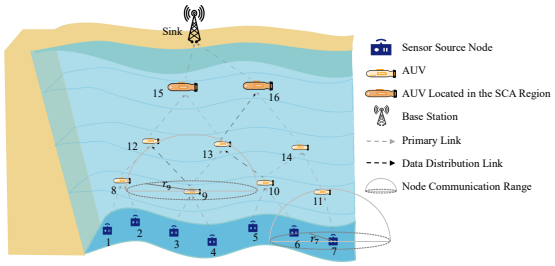


Fig. 1: Schematic of the system model.

The HUWSN satisfies following assumptions:

1) The wide and uniform distribution of AUVs at each layer ensures multiple transmission paths to $Sink$ in the network, reducing the occurrence of dead zones, so the HUWSN is connective.
2) Positions of the sensor source nodes, AUVs, and $Sink$ are known. They are equipped with positioning systems

to determine their own locations as well as those of nodes within their communication range.

3) The accidental failure of AUVs is not taken into consideration because they possess excellent performance. Furthermore, as AUVs within the SCA are subjected to high loads, AUVs deployed near the $Sink$ have initial energy levels greater than the other AUVs.

However, it should be noted that these assumptions also have certain limitations in practical applications. Firstly, environmental factors such as ocean currents, obstacles, and unpredictable movements of marine organisms can disrupt the planned deployment of AUVs, making it challenging to achieve the ideal multiple transmission paths and connectivity. Moreover, mechanical failures, power supply issues, or collisions with other objects can occur, which can disrupt the network operation. This model is not suitable for highly dynamic and unpredictable environments. For instance, regions with high obstacle density or interference risks for positioning systems see poor performance.

The sensor source node $i \in \mathcal{I}$ can be formalized as triples $< r_i, F_i, H_i >$, where $r_i$ represents the communication radius, $F_i$ represents the amount of data transmitted, and $H_i = (x_i, y_i, z_i)$ represents the position coordinate. AUV $a \in \mathcal{A}$ is denoted by $< r_a, E_a^0, H_a >$, where $r_a$ represents the communication radius, $E_a^0$ represents the initial energy, and $H_a = (x_a, y_a, z_a)$ represents the position coordinate. The coordinate of the $Sink$ is $(X, Y, 0)$.

*Definition 1:* The adjacent nodes of node $u \in \mathcal{I} \cup \mathcal{A}$ [2] are defined as nodes that can directly communicate with $u$. For $u$ in the HUWSN, $j$ is considered an adjacent node of $u$ if and only if $D_{u,j} \leq r_u$.

Where $D_{u,j}$ represents the Euclidean distance between $u$ and $j$, and $r_u$ represents the communication radius of $u$. The set of adjacent nodes of node $u$ is denoted as $\mathcal{J}_u = \{1, \cdots, j, \cdots, \mid \mathcal{J}_u \mid\}$, $\mathcal{J}_u \subset \mathcal{A}$, where $\mid \mathcal{J}_u \mid$ represents the number of elements in $\mathcal{J}_u$.

*Definition 2:* Nodes in $\mathcal{J}_u$ responsible for forwarding packets from node $u$, are defined as next-hop relay nodes of node $u$.

Since packets may be split and transmitted along multiple paths, the next-hop relay node of node $u$ can be multiple. The set of next-hop relay nodes of node $u$ is denoted as $\mathcal{V}_u = \{1, \cdots, v, \cdots, \mid \mathcal{V}_u \mid\}$, $\mathcal{V}_u \subset \mathcal{J}_u$, where $\mid \mathcal{V}_u \mid$ represents the number of elements in $\mathcal{V}_u$.

**Link Transmission Model.** Let $W_{u,v}$ be the packet sent by node $u$ to node $v \in \mathcal{V}_u$, formalized as $< F_{u,v}, L_{u,v} >$, where $F_{u,v}$ represents the size of the packet and $L_{u,v}$ denotes the communication link between node $u$ and node $v$. To prevent the overloading of some links and achieve load balancing in HUWSN, a reasonable transmission model needs to be designed. The load $\Gamma_{u,v}$ on a link $L_{u,v}$ can be calculated as the ratio between the actual transmitted packet size and the maximum packet size that can be transmitted, expressed as follows:

$$\Gamma_{u,v} = \frac{F_{u,v}}{B_{u,v} T_{u,v}} \tag{1}$$

where $B_{u,v}$ is the bandwidth of the link $L_{u,v}$, indicating the amount of data that can be transmitted per unit of time. $T_{u,v}$ is the transmission delay, $T_{u,v} = F_{u,v}/R_{u,v}$, and the transmission rate $R_{u,v}$ can be expressed as follows:

$$R_{u,v} = B_{u,v} \log_2 (1 + \frac{P_u^t D_{u,v}}{B_{u,v} N_0}) \tag{2}$$

where $P_u^t$ represents the transmit power and $N_0$ denotes the noise power density.

Eq.1 represents the proportion of actual transmitted packet size within the capacity of the link. If the ratio is greater than 1, it indicates that the actual transmitted packet size is exceeds the capacity of the link, leading to an excessive link load. Conversely, it means that the actual transmitted packet size does not take up the full capacity of the link, and the load of the link is lower.

**Energy Consumption Model.** The energy consumption of the relay node is primarily attributed to communication, which includes receiving and sending data [17]. When AUV $v$ receives the packet $W_{u,v}$ from node $u$ and forwards the data to the next-hop node $w$, its energy consumption depends on factors such as packet size, transmission power, and distance:

$$E_v = P_v^r \sum_{u \in \mathcal{I} \cup \mathcal{A}} \frac{F_{u,v}}{R_{u,v}} + P_v^t T_{v,w} \tag{3}$$

where the first term represents the energy consumed for receiving data, while the second term represents the energy consumed for sending data. $P_v^r$ and $P_v^t$ denote the receiving power and the sending power respectively. $\sum_{u \in \mathcal{I} \cup \mathcal{A}} F_{u,v}/R_{u,v}$ represents the total time consumption of node $v$ in receiving data.

### B. Problem Description

Considering the performance characteristics of nodes, the network load balancing can be achieved by a suitable route allocation scheme, which includes:

1) Given the spatial distribution of AUVs, formulate the optimal routing choice $\Pi_i = (i, v_1, \cdots, v_s, Sink)$ for sensor source node $i$ to construct the initial network topology. Where $i$ represents the starting node of the path, $(v_1, \cdots, v_s)$ represents intermediate nodes, and $Sink$ is the destination. The goal is to homogenize the size of packets forwarded by nodes at each layer. The energy consumption of a relay node increases proportionally with its involvement in packet forwarding. Thus the above objective is formally defined as minimizing the energy consumption variance of nodes at each layer. Nodes at the $h$-th layer can be denoted as $\mathcal{M}_h$, $m \in \mathcal{M}_h$. The energy consumption variance among nodes at the $h$-th layer $\sigma_h$ is expressed in Eq.4.

$$\min \sigma_h = \frac{1}{\mid \mathcal{M}_h \mid} \sum_{m \in \mathcal{M}_h} (E_m - \overline{E})^2 \tag{4}$$

where $E_m$ represents the energy consumption of node $m$, $\overline{E}$ represents the average of the energy consumption of nodes in

[2]In the following, we use $u$ to denote a node in the network, $j$ to denote an adjacent AUV of $u$ instead of $a$, and $v$ to denote a relay AUV instead of $a$.

this layer, and $\mid \mathcal{M}_h \mid$ represents the number of elements in $\mathcal{M}_h$.

2) To optimize the link load balance, the data allocation policy $\Phi_u = (\mathcal{V}_u, \mathcal{F}_{u,v})$ for node $u$ is formulated. Each node $v$ in $\mathcal{V}_u = \{1, \cdots, v, \cdots, \mid \mathcal{V}_u \mid\}$ is assigned the packet $W_{u,v}$ corresponding to a packet size of $F_{u,v}$, where $\mathcal{F}_{u,v} = \{F_{u,1}, \cdots, F_{u,v}, \cdots, F_{u,|\mathcal{V}_u|}\}$. The objective is formally defined as minimizing the network link load variance. Specifics are as follows:

$$\min \sigma = \frac{1}{O} \sum_{u \in \mathcal{I} \cup \mathcal{A}, v \in \mathcal{V}_u} \left(\Gamma_{u,v} - \overline{\Gamma}\right)^2 \tag{5}$$

$$\sum_{u \in \mathcal{I} \cup \mathcal{A}, v \in \mathcal{V}_u} F_{u,v} = F_u \tag{6}$$

$$\mid \mathcal{V}_u \mid > 1, \forall u \in \mathcal{I} \cup \mathcal{A} \tag{7}$$

In Eq.5, $\sigma$ denotes the network link load variance, $O$ represents the total number of links in the network, and $\overline{\Gamma}$ is the average value of the links load. The smaller the $\sigma$ is, the more balanced each link's load will be. Eq.6 indicates that the total size of packets allocated to each node in $\mathcal{V}_u$ is equal to the size of the data sent by node $u$. Eq.7 ensures that every node has a certain number of next-hop relay nodes forwarding data for it.

## IV. Hierarchical Route Allocation Mechanism

In this section, HRAM is proposed to achieve load balancing across the network. The mechanism consists of three modules: initial network topology, data allocation, and route allocation optimization. Specific details of modules are described in following subsections.

### A. Initial Network Topology Phase of HRAM

Each node has multiple path to reach the $Sink$. To ensure that the number of relay tasks undertaken by each layer of AUVs is similar, the proposed Balanced Routing Selection Algorithm (BRSA) selects a next-hop relay node for each node based on the evaluation value and path counter. Finally, an initial network topology is formed, providing a solid foundation for subsequent data allocation optimization.

The evaluation function $\varphi_j$ denotes the state of each adjacent AUV $j$, as shown in Eq.8. The energy factor $e_j$ measures the residual energy of AUV $j$. $\alpha$ and $\gamma$ represent weighting coefficients. Regardless of the distance of the node to $Sink$, $\varphi_j$ will become very low, i.e., 0.0001, when the residual energy of node $j$ is less than or equal to the average residual energy of nodes in $\mathcal{J}_u$. This prevents the node from being too low in energy and thus dying prematurely. Node $u$ selects AUV $j$ as the next-hop relay node only if $\varphi_j$ satisfies the state threshold $\varphi_u^{req}$, $\varphi_j \geq \varphi_u^{req}$.

$$\varphi_j = \begin{cases} \alpha e_j + (1-\alpha)\frac{D_{u,\mathrm{Sink}}}{D_{j,\mathrm{Sink}}} + \frac{\gamma}{D_{u,j}}, & E_j^0 - E_j > \frac{1}{|\mathcal{J}_u|}\sum_{j \in \mathcal{J}_u} E_j^0 - E_j \\ 0.0001, & \text{otherwise} \end{cases} \tag{8}$$

$$e_j = \frac{E_j^0 - E_j}{E_j^0} \tag{9}$$

Compared with other routing algorithms, BRSA designs a path counter $path_j$ for each adjacent node $j$. When a node is identified as a relay node, its path counter value increases by 1. It carefully considers the capabilities and load-bearing potential of each node. By doing so, it avoids the pitfall of overburdening nodes within the same layer. The BRSA is presented in Algorithm 1.

**Algorithm 1** BRSA

**Input:** $\mathcal{I}$, $\mathcal{A}$ and $Sink$
**Output:** Best routing option to reach base station $\Pi_i$

```
for i ∈ I do
    s ← i , Π_s ← {s}, V_u ← ∅
    while s ≠ Sink do
        if Sink ∉ J_s then
            for each adjacent node j, j ∈ J_s do
                Calculate φ_j according to Eq.8,9
                if φ_j ≥ φ_s^req then
                    V_s ← V_s ∪ {j}
                end if
            end for
            for each relay node v, v ∈ V_s do
                Compare the path counter Path_v
                if Path_v is equal, ∀v ∈ V_s then
                    Next-hop relay node is v_1 with the largest value of φ_{v_1}
                    Π_s ← Π_s ∪ {v_1}, Path_{v_1} ← Path_{v_1} + 1
                else
                    Next-hop relay node is v_2 with the the least value of Path_{v_2}
                    Π_s ← Π_s ∪ {v_2}, Path_{v_2} ← Path_{v_2} + 1
                end if
            end for
        else
            Π_s ← Π_s ∪ {Sink}
        end if
        s ← the selected next-hop relay node
    end while
end for
return Π_i
```

### B. Data Allocation Phase of HRAM Based on Load Factor

In HUWSN, packets sent by sensor source nodes are of different sizes, and larger packets will take up more link capacity during transmission. Excessive load on some links can easily cause data transmission errors or packet loss. Data Allocation Algorithm based on load factor (DAA) is proposed on the basis of initial network topology.

The proposed DAA is presented in Algorithm 2. When $F_u - F_u^{avg} \geq \theta$, node $u$ splits the packet to send, where $F_u^{avg}$ is the average packet size loaded by node $u$, and $\theta$ is the traffic load threshold. For $v, v \in \mathcal{V}_u$, the allocated packet size $F_{u,v}$ can be expressed as follows:

$$\rho_v = \eta e_v + (1-\eta)\frac{B'_{u,v}}{B_{u,v}} \tag{10}$$

$$F_{u,v} = \begin{cases} F_u \rho_v / \sum_{v=1}^{|\mathcal{V}_u|} \rho_v, & v = 1, 2, \cdots, \mid \mathcal{V}_u \mid -1 \\ F_u - \sum_{v=1}^{|\mathcal{V}_u|-1} F_{u,v}, & v = \mid \mathcal{V}_u \mid \end{cases} \tag{11}$$

where $\rho_v$ represents the load factor, measuring the load condition of node $v$ and the transmission link $L_{u,v}$. $B'_{u,v}$ denotes the available bandwidth of the link. $\eta$ represents the adjusting parameter, $\eta \in (0,1)$.

**Algorithm 2** DAA

**Input:** $\mathcal{I}$, $\mathcal{A}$, and $Sink$
**Output:** $\Phi_u = (\mathcal{V}_u, \mathcal{F}_{u,v})$

**for** $u \in \mathcal{I} \cup \mathcal{A}$ **do**
  **if** $F_u - F_u^{avg} \geq \theta$, $Sink \notin \mathcal{J}_u$ **then**
    Initialize set $\mathcal{V}_u \leftarrow \emptyset$
    **for** each adjacent node $j$, $j \in \mathcal{J}_u$ **do**
      Calculate $\varphi_j$ according to Eq.8,9
      **if** $\varphi_j \geq \varphi_u^{req}$ **then**
        $\mathcal{V}_u \leftarrow \mathcal{V}_u \cup \{j\}$
      **end if**
    **end for**
    **for** each relay node $v, v \in \mathcal{V}_u$ **do**
      Calculate $\rho_v, F_{u,v}$ according to Eq.10,11
    **end for**
  **end if**
**end for**
**return** $\Phi_u = (\mathcal{V}_u, \mathcal{F}_{u,v})$

### C. Route Allocation Optimization Phase of HRAM

The Heuristic Route Allocation Optimization Algorithm (HRAOA) utilizes an improved adaptive genetic algorithm to optimize the network's link load.

**Algorithm 3** HRAOA

**Input:** The node $u$ sending data, $\mathcal{J}_u$, and the maximum number of iterations max_gen

**for** $u \in \mathcal{I} \cup \mathcal{A}$ **do**
  **if** $\mathcal{J}_u \neq \emptyset$ **then**
    Randomly select nodes in $\mathcal{J}_u$ as the relay nodes
    Allocate data based on the load factor
  **end if**
**end for**
population $= \{1, \cdots, g \cdots, G\}$, $Global\_best \leftarrow \emptyset$, $\lambda'_{\max} \leftarrow -\infty$
**for** gen $= 1$ *to* max_gen **do**
  Calculate $\lambda'_g$, and select individual $g$ with the largest fitness value
  **if** $Global\_best = \emptyset$ **or** $\lambda'_g > \lambda'_{\max}$ **then**
    $Global\_best \leftarrow g$
    $\lambda'_{\max} \leftarrow \lambda'_g$
  **else**
    Roulette wheel selection
    Crossover operation
    Mutation operation
  **end if**
**end for**

**Genetic Coding Design**. Each individual is represented by the matrix structure. The first row of the matrix identifies the index of each node sending data. Other rows are encoded with real numbers, where the integer part indicates the relay node index and the fractional part indicates the packet size. To maintain the integrity of the matrix, extra rows are added accordingly and padded with zeros if a node contains multiple relay node. For instance, in Fig.2(a), there are five nodes sending data. Node 1 sends a packet of size 3 to node 6. Node 2 sends a packet of size 2 to node 6 and another packet of size 4 to node 7. As node 1 only has one relay node, the last row of the first column of the code is therefore 0.

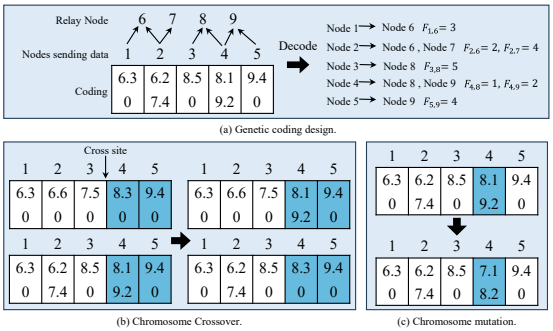


Fig. 2: Schematic of chromosome operations.

**Adaptation Function.** In this paper, we design the fitness function $\lambda_g$ for individual $g$ as the load variance $\sigma$ of the link, $\lambda_g = \sigma$, which is calculated by Eq.5. To enhance competitiveness within the population, we design an improved fitness function $\lambda'_g$, which consists of $\lambda_g$ and the $Sigmoid$ function, $\lambda'_g \in (0,1)$. The formula for calculating $\lambda'_g$ can be expressed as follows:

$$\lambda'_g = \begin{cases} \frac{1}{1+\exp((\lambda_g - \lambda_{avg})/(\lambda_{\max} - \lambda_{avg}))}, & \mu \geq 30\%G \\ \frac{1}{1+\exp(\lambda_g - \lambda_{avg})}, & \mu < 30\%G \end{cases} \tag{12}$$

Where $\lambda_{avg}$ represents the mean of $\lambda_g$ in the contemporary population, and $\lambda_{max}$ represents the maximum of $\lambda_g$ in the contemporary population. To prevent more individuals with $\lambda'_g$ close to 1 or 0, which will lead to poor competitiveness, we add the judgment. $\mu$ denotes the number of individuals whose $\lambda'_g$ close to 1 or 0, and $G$ is the magnitude of the population size.

**Genetic Operators. 1) Roulette Wheel Selection Operator.** The selection is based on probability, associated with its fitness. The number of times the wheel rotates is equal to the population size $G$.

$$P_g^{select} = \lambda'_g / \sum_{g=1}^{G} \lambda'_g \tag{13}$$

**2) Crossover Operator.** The crossover operation on individual $g$ is performed according to the crossover probability $P_g^{cross}$ to produce new individuals. The crossover operation is shown in Fig.2(b). The crossover probability can be expressed in Eq.14, where $\lambda'_{max}$ and $\lambda'_{avg}$ represent the maximum fitness value and the average fitness value in the parent generation, respectively.

$$P_g^{cross} = \begin{cases} \frac{k_1(\lambda'_{max} - \lambda'_g)}{\lambda'_{max} - \lambda'_{avg}} & \lambda'_g > \lambda'_{avg} \\ k_1 & \lambda'_g \leq \lambda'_{avg} \end{cases} \tag{14}$$

**3) Mutation Operator.** As shown in Fig.2(c), randomly generate the index of the replacement node among its adjacent nodes. The mutation probability $P_g^{mutate}$ can be expressed as follows:

$$P_g^{muatate} = \begin{cases} \frac{k_2(\lambda'_{max}-\lambda'_g)}{\lambda'_{max}-\lambda'_{avg}} & \lambda'_g > \lambda'_{avg} \\ k_2 & \lambda'_g \leq \lambda'_{avg} \end{cases} \quad (15)$$

## V. Experimental Results and Analysis

### A. Experimental Setup

The effectiveness of the HRAM is verified through experiments. The experiments are run in Python 3.12. The computer processor and memory parameters were 13th Gen Intel(R) Core(TM) i9-13900HX, 2.20 GHz and 16GB RAM. Unless otherwise stated, experiment parameters are shown in Table I.

TABLE I: Experimental simulation parameters.

| Parameter | Value |
|---|---|
| Packet size sent by each sensor source node (KB) | $F_i \in [30, 100]$ |
| Maximum communication distance (m) | $r_i \in [100, 200]$ and $r_a \in [100, 200]$ |
| Transmit/Receive power (mW) | $P_u{}^t = 60$ and $P_u{}^r = 60$ |
| Link bandwidth (KHz) | $B_{u,v} = 1$ |
| Noise power density (W/Hz) | $N_0 = 1$ |
| Initial energy of AUV (KJ) | 1 |
| Initial energy of AUV in SCA (KJ) | 2 |
| Traffic load threshold (KB) | $\theta = 10$ |
| Coefficients | $\alpha = 0.4, \gamma = 0.3, k_1 = 0.8, k_2 = 0.01$ |

We consider the packet size sent by each sensor source Node within a specific time interval is from 30 KB to 100 KB. In practical scenarios where sensors typically send data at varying frequencies, influenced by the characteristics of the monitored environment and the data sampling rate. This range successfully simulates various environmental monitoring situations. The maximum communication distance is from 100 m to 200 m, which often require effective communication over relatively short distances. The transmit and receive power are 60 mW because of the relatively fast attenuation of sound waves traveling through water. The initial energy of AUVs is 1 KJ. setting the initial energy of AUVs in the SCA area to 2 KJ reflects the advantages of proximity to the base station. The traffic load threshold is 10 KB. Implementing this limit is crucial for maintaining network stability and ensuring efficient data transmission. The coefficients are taken for the best results of the experiment.

### B. Comparative Experimental Analysis

Our experimental results are based on 500 rounds of randomly generated simulation scenarios, and the average of the experimental results is taken.

**Initial Network Topology Formation.** In the experiment, five layers are set in the scene. The first layer comprises 10 sensor source nodes. The initial network topology formed by HRAM-BRSA is shown in Fig. 3(a). Taking sensor source node 1 as an example, its optimal routing to reach the $Sink$ is $\Pi_1 = (1, 11, 16, 19, 21)$.

After a single round of data transmission from the sensor source nodes, compared with the Dijkstra algorithm [18], the distribution of energy consumed by each AUV is analyzed, as shown in Fig.3(b). AUVs 16-18 (located in the third layer) consume almost equal amounts of energy. The energy consumption of AUV 19 and AUV 20 is more balanced than that of the Dijkstra algorithm. Due to the aggregation characteristic of HUWSN, nodes closer to $Sink$ (AUV 19 and 20) carry more data, resulting in higher consumption. This is why we consider using the heterogeneous AUVs.

The variance of the energy consumption of AUVs in each layer is shown in Table II, from which it can be seen that the variance by HRAM-BRSA is smaller than that by the Dijkstra algorithm. Indicating that HRAM-BRSA reduces the difference in energy consumption of nodes at each layer.

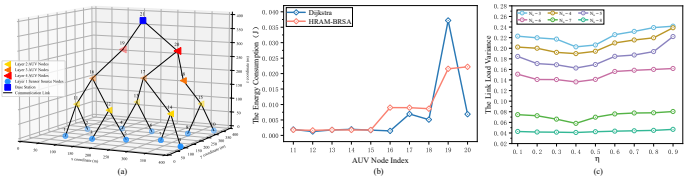


Fig. 3: (a) Schematic of the initial network topology. (b) Schematic of the distribution of energy consumption. (c) Schematic of the link load variance under different $\eta$ in the network.

TABLE II: Comparison of energy consumption variance of each layer.

| Layer number | Algorithm | |
|---|---|---|
| | Dijkstra | HRAM-BRSA |
| 1 | $6.71 \times 10^{-8}$ | $3.16 \times 10^{-9}$ |
| 2 | $5.2 \times 10^{-6}$ | $2.58 \times 10^{-8}$ |
| 3 | $2.3 \times 10^{-4}$ | $1.02 \times 10^{-7}$ |

**Route Allocation Performance Analysis.** Inspired by the study [16], this experiment only focuses on the data transmission between two layers in the scenario, namely referred to as the sending and receiving layers. By altering the parameter $\eta$ (ranging from 0.1 to 0.9), we observe the variation of link load variance with different quantities of AUVs in the receiving layer, denoted as $N_a$. The result is shown in the Fig.3(c). It is observed that at $\eta = 0.4$, the load variance is minimized across various quantities of AUVs. Therefore, in the subsequent experiments, we set $\eta = 0.4$ to validate the performance of HRAM.

**1) Load Balancing.** The results of HRAM-HRAOA are compared with the Genetic Algorithm (GA) [19] and Weighted Round Robin (WRR) [20]. The experimental setup involves setting the number of nodes in the sending layer to 10, while adjusting the quantity of AUVs in the receiving layer. A comparison of link load variance between two layers is illustrated in Fig.4(a). With an increase in the number of AUVs, all three algorithms show a decreasing trend in load variances. Compared to the other two algorithms, HRAM-HRAOA exhibits a smaller load variance, balancing the distribution of data across the link.

**2) Total Network Energy Consumption.** In the scenario where the number of sending layer nodes is 10, and the number of AUVs in the receiving layers is adjusted to analyze the change in the total energy consumption of these 10 nodes. The total energy consumption of the sending layer nodes increases as the number of relay nodes increases, because nodes split more packets for transmission, increasing the number of packet

transfers. As can be seen from Fig.4(b), HRAM-HRAOA exhibits relatively small total energy consumption compared to the other two algorithms, which proves that the proposed mechanism can effectively reduce overall energy consumption of nodes.

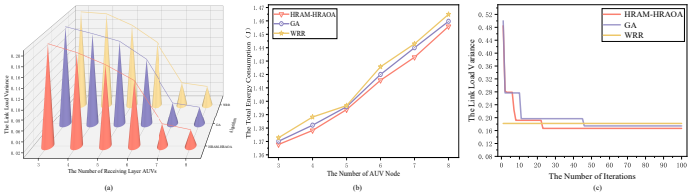


Fig. 4: (a) Schematic of the link load variance. (b) Schematic of the total network energy consumption. (c) Schematic of the algorithm convergence.

**3) Convergence Performance.** The convergence performance of the HRAM-HRAOA is shown in Fig.4(c) in a scenario where the number of nodes in the sending layer is 10 and the number of AUVs in the receiving layer is 5. HRAM-HRAOA reaches its optimal variance value when the number of iterations reaches about 23 times. By designing an improved fitness function and genetic operator, the algorithm achieves a more stable load variance within a relatively small number of iterations, proving the fast convergence of the algorithm.

## VI. Summary

The proposed HRAM provided a load-balanced routing scheme. By constructing the initial network topology and designing a route allocation strategy based on the state of nodes and links, the load variance in the network was reduced. Experiment results show that HRAM-BRSA outperforms the Dijkstra algorithm in terms of energy balancing of nodes in routing. When compared to GA and WRR, HRAM-HRAOA effectively reduces the load variance at the same node size, enhancing network performance and dependability.

## References


[1] M. Jahanbakht, W. Xiang, L. Hanzo, and M. Rahimi Azghadi, "Internet of underwater things and big marine data analytics—a comprehensive survey," *IEEE Communications Surveys & Tutorials*, vol. 23, no. 2, pp. 904–956, 2021.

[2] T. Qiu, Z. Zhao, T. Zhang, C. Chen, and C. L. P. Chen, "Underwater internet of things in smart ocean: System architecture and open issues," *IEEE Transactions on Industrial Informatics*, vol. 16, no. 7, pp. 4297–4307, 2020.

[3] W. Liang, Y. Hu, N. Kasabov, and V. Feigin, "Exploring associations between changes in ambient temperature and stroke occurrence: Comparative analysis using global and personalised modelling approaches," in *Neural Information Processing*. Springer Berlin Heidelberg, 2011, pp. 129–137.

[4] I. Jawhar, N. Mohamed, J. Al-Jaroodi, and S. Zhang, "An architecture for using autonomous underwater vehicles in wireless sensor networks for underwater pipeline monitoring," *IEEE Transactions on Industrial Informatics*, vol. 15, no. 3, pp. 1329–1340, 2019.

[5] Z. Zhao, C. Liu, Z. Li, B. Wu, M. Ma, Z. Zhao, and L. Liu, "Ebtcor: an energy-balanced 3d topology control algorithm based on optimally rigid graph in uwsns," *Ad Hoc & Sensor Wireless Networks*, vol. 42, no. 3-4, pp. 295–315, 2018.

[6] E. Felemban, F. K. Shaikh, U. M. Qureshi, A. A. Sheikh, and S. B. Qaisar, "Underwater sensor network applications: A comprehensive survey," *International Journal of Distributed Sensor Networks*, vol. 11, no. 11, p. 896832, 2015.

[7] A. Naushad, G. Abbas, S. Shah, and Z. Abbas, "Energy efficient clustering with reliable and load-balanced multipath routing for wsns," 02 2020, pp. 1–9.

[8] C.-M. Yu, M.-L. Ku, L.-C. Wang, F.-H. Huang, and W.-K. Jia, "Bratra: Balanced routing algorithm with transmission range adjustment for energy efficiency and utilization balance in wsns," *IEEE Internet of Things Journal*, vol. 10, no. 2, pp. 1096–1111, 2023.

[9] B. Shu, C. Li, Y. Shi, H. Wang, and H. Li, "A 3d uwb hybrid localization method based on bsr and l-aoa," in *Neural Information Processing*. Singapore: Springer Nature Singapore, 2024, pp. 3–15.

[10] S. Ibrahim, J. Liu, M. Al-Bzoor, J.-H. Cui, and R. Ammar, "Towards efficient dynamic surface gateway deployment for underwater network," *Ad Hoc Networks*, vol. 11, no. 8, pp. 2301–2312, 2013.

[11] M. Arifuzzaman, M. Matsumoto, and T. Sato, "An intelligent hybrid mac with traffic-differentiation-based qos for wireless sensor networks," *IEEE Sensors Journal*, vol. 13, no. 6, pp. 2391–2399, 2013.

[12] W. Zhang, J. Wang, G. Han, Y. Feng, and X. Tan, "A nonuniform clustering routing algorithm based on a virtual gravitational potential field in underwater acoustic sensor network," *IEEE Internet of Things Journal*, vol. 10, no. 15, pp. 13 814–13 825, 2023.

[13] Z. Zhao, C. Liu, X. Guang, and K. Li, "Mlrs-rl: An energy-efficient multilevel routing strategy based on reinforcement learning in multi-modal uwsns," *IEEE Internet of Things Journal*, vol. 10, no. 13, pp. 11 708–11 723, 2023.

[14] Q. Wang, J. Li, Q. Qi, P. Zhou, and D. O. Wu, "A game-theoretic routing protocol for 3-d underwater acoustic sensor networks," *IEEE Internet of Things Journal*, vol. 7, no. 10, pp. 9846–9857, 2020.

[15] X.-H. Lin, Y.-K. Kwok, H. Wang, and N. Xie, "A game theoretic approach to balancing energy consumption in heterogeneous wireless sensor networks," *Wireless Communications and Mobile Computing*, vol. 15, no. 1, pp. 170–191, 2015.

[16] J. Zhang, X. Wang, B. Wang, W. Sun, H. Du, and Y. Zhao, "Energy-efficient data transmission for underwater wireless sensor networks: A novel hierarchical underwater wireless sensor transmission framework," *Sensors*, vol. 23, no. 12, 2023.

[17] Z. Liu, X. Meng, Y. Liu, Y. Yang, and Y. Wang, "Auv-aided hybrid data collection scheme based on value of information for internet of underwater things," *IEEE Internet of Things Journal*, vol. 9, no. 9, pp. 6944–6955, 2022.

[18] M. Tang, J. Sheng, and S. Sun, "A coverage optimization algorithm for underwater acoustic sensor networks based on dijkstra method," *IEEE/CAA Journal of Automatica Sinica*, vol. 10, no. 8, pp. 1769–1771, 2023.

[19] D.-g. Zhang, S. Liu, X.-h. Liu, T. Zhang, and Y.-y. Cui, "Novel dynamic source routing protocol (dsr) based on genetic algorithm-bacterial foraging optimization (ga-bfo)," *International Journal of Communication Systems*, vol. 31, no. 18, p. e3824, 2018.

[20] X. Tan, X. Li, Z. Liu, and Y. Ding, "Burst traffic awareness wrr scheduling algorithm in wide area network for smart grid," in *Communications and Networking*. Springer International Publishing, 2020, pp. 117–128.